Nonlinear Gain Position Control Using Only Position Feedback for Permanent Magnet Stepper Motors

Wonhee Kim, *Member, IEEE*, Youngwoo Lee, Donghoon Shin, and Chung Choo Chung, *Member, IEEE*

***Abstract*—This article proposes a robust nonlinear position control for permanent magnet stepper motors. We develop a new single-input single-output model that consists of position, velocity, and acceleration using a commutation scheme to lump a system function and an external disturbance into a disturbance. An augmented observer is designed to estimate the position, velocity, acceleration, and disturbance. Because the disturbance refers to external disturbance, acceleration dynamics, and parameter uncertainties, it is difficult to accurately estimate disturbance without the high observer gain. It may result in the degradation of the position tracking performance. The nonlinear controller is then developed using backstepping to suppress the position tracking error using the input-to-state stability property. The key innovation of the proposed method is the design of the nonlinear gain to suppress the position tracking error according to the disturbance estimation error. Thus, the use of the high observer gain to accurately estimate the disturbance can be avoided. The proposed control algorithm was experimentally verified using the PM stepper motor control system and can be easily implemented in real-time using position measurements only.**

***Index Terms*—Backstepping, nonlinear gain, permanent magnet stepper motor, position tracking.**

NOMENCLATURE

θ	Rotor (angular) position [rad].
ω	Rotor (angular) velocity [rad/s].
i_a and i_b	Currents of phases A and B [A].
v_a and v_b	Voltages of phases A and B [V].
B	Viscous friction coefficient [N · m·s/rad].
J	Inertia of the motor [Kg · m^2].
K_m	Motor torque constant [N · m/A].
R	Resistance of phase winding [Ω].
L	Inductance of phase winding [H].
τ_l	Load torque perturbation [N · m].
N_r	Number of rotor teeth.
k_1, k_2, k_3, k_{3_a}, k_{3_b}, ν_1, and ν_2	Control gains.
l_1, l_2, l_3, and l_4	Observer gains.

Manuscript received August 13, 2020; revised October 31, 2020; accepted December 19, 2020. Date of publication December 25, 2020; date of current version March 5, 2021. This work was supported by the Research Program, Improved Development of an Electric Power Steering System (EPS) to enhance the driving stability of microelectric vehicle (20007447), funded by the Ministry of Trade, Industry, and Energy (MOTIE, Korea). Recommended for publication by Associate Editor U. Deshpande. *(Corresponding author: Youngwoo Lee.)*

Wonhee Kim is with the School of Energy Systems Engineering, Chung-Ang University, Seoul 06974, South Korea (e-mail: whkim79@cau.ac.kr).

Youngwoo Lee is with the Department of Electrical Engineering, Chonnam National University, Gwangju 61186, South Korea (e-mail: stork84.lee@gmail.com).

Donghoon Shin is with the Global R&D Center, MANDO Corporation, Seongnam 463400, South Korea (e-mail: donghoon.shin@halla.com).

Chung Choo Chung is with the Division of Electrical and Biomedical Engineering, Hanyang University, Seoul 04763, South Korea (e-mail: cchung@hanyang.ac.kr).

Color versions of one or more figures in this article are available at https://doi.org/10.1109/TPEL.2021.3046849.

Digital Object Identifier 10.1109/TPEL.2020.3046849

I. INTRODUCTION

PERMANENT magnet (PM) stepper motors have been widely used for positioning applications due to power density, high efficiency, their durability, high torque to inertia ratio, and the absence of rotor winding [1]. In industrial applications, microstepping is widely used with a closed-loop in current-loops, thus, proportional-integral (PI) controllers are embedded in the motor drives for current regulations [2]. However, as the microstepping-based control method with current controller considered only electrical dynamics in the PM stepper motors, a position tracking error during the nonzero velocity period cannot be avoided [3].

With the increase in power and decrease in cost of embedded processors in recent years, drives and control systems for PM stepper motor have become increasingly sophisticated. Thus, for positioning applications, PM stepper motor can be substituted for expensive servo motors such as PM synchronous motors as a cheaper replacement in closed-loop operation. Various controllers have been proposed for the improvement of the position/velocity control performance in PM stepper motors [3]–[11]. A nonlinear controller using a field weakening control (FWC) was presented for the improvement of position control [4]. A simple and effective position and velocity controller was proposed for FWC of the PMSMs [5]. In [6], a sensorless controller was proposed for the velocity control of the PMSMs. In [7], torque modulation based microstepping was developed to realize field oriented control (FOC) and FWC without direct-quadrature (DQ) transformation, and an integrator reset control was designed in [8] to improve the transient response with position control of the PM stepper motor. An enhanced nonlinear damping controller was proposed to reduce the position tracking error [9]. Furthermore, a nonlinear H_2 control with varying linear parameters was developed to optimize the control performance [10]. In [11], an effective closed-loop control that consists of motor parameter identification, closed-loop current control, closed-loop position control, and damping control was proposed. A model predictive controller was designed for external periodic disturbances attenuation in the PMSM [12]. An internal model

principle-based controller was proposed to reduce sideband harmonics for the PMSM with low switching frequency inverters in [13].

However, although these methods improved the position/velocity performance, the effects of parameter uncertainties and the unknown load torque were not considered in controller design. To solve these problems, various approaches have been researched such as neural network based adaptive controller [11], robust and/or adaptation methods [14]–[16], robust adaptive nonlinear dynamic controller [17], and high-order sliding-mode controller [18]. A disturbance observer based control method was proposed for the FWC of the PMSMs [19]. Nevertheless, the above-mentioned methods also have limitations in that they require information about full state feedback, variation ranges and/or nominal values of the parameters to estimate parameters.

From this perspective, augmented observers (AOB) is a very effective method to estimate disturbances including external disturbances and/or system uncertainties [20]–[22]. However, although AOB-based control methods make nonlinear systems robust to external disturbances and system uncertainties, in reality, it is difficult to precisely estimate disturbances if they include system uncertainties or if they vary rapidly. Therefore, the estimation error of the disturbance may become large and degrade the position tracking performance. To reduce the estimation error of the disturbance, the bandwidth of the observer needs to be increased; however, high gain for the wider bandwidth of the AOB may amplify measurement noise. Furthermore, there is an assumption with these methods that either the system uncertainties or the full state are bounded.

In addition, the PM stepper motor is a fourth order two-input single-output (TISO) nonlinear system due to its dynamic characteristics. The model of the PM stepper motor consists of mechanical (position and velocity) dynamics and electrical (current) dynamics. Previous methods are designed based on the cascade control concept for both current and position tracking, where currents track the desired currents that generate the torque required by the electrical controller and the position tracker tracks the position required by the mechanical controller. Therefore, the structures of the previous methods (the controllers, observers, and adaptation methods) are necessarily complex.

In this article, we propose a robust nonlinear position control for PM stepper motors. This innovative approach to position control is not based on the cascade control concept. We develop new single-input single-output (SISO) model that consists of position, velocity, and acceleration using a commutation scheme to lump a system function and an external disturbance into a disturbance. An AOB is designed to estimate the position, velocity, acceleration, and disturbance. However, as disturbance refers to external disturbance, acceleration dynamics, and parameter uncertainties, making an accurate estimation of it is extremely difficult without high observer gain for the wider bandwidth. The poor disturbance estimation performance may result in the degradation of the position tracking performance. The nonlinear controller is then developed using backstepping to suppress the position tracking error using the input-to-state stability (ISS) property. The key innovation of the proposed method is the design of the nonlinear gain to suppress the position tracking error according to the disturbance estimation error. Thus the use of the high observer gain to accurately estimate the disturbance can be avoided. Results confirm that it is not necessary to account for very small estimation errors to realize precise output tracking when using the input-to-state stability (ISS) property without the assumption that the full state is bounded. The stability of the closed loop including the PM stepper motor, controller, and observer is then mathematically demonstrated. The proposed method is robust to the external disturbance and parameter uncertainties. This approach simplifies the design process so that the control algorithm is suitable for real time control. The performance of the proposed method is validated via simulations and experiments.

II. PM Stepper Motor Model and Problem Formulation

A. Mathematical Model of PM Stepper Motor

The dynamics of the PM stepper motor can be represented as follows [7]

$$\begin{aligned}
\dot{\theta} &= \omega \\
\dot{\omega} &= \frac{1}{J}[-K_m i_a \sin(N_r\theta) + K_m i_b \cos(N_r\theta) - B\omega - \tau_l] \\
\dot{i}_a &= \frac{1}{L}[v_a - Ri_a + K_m\omega \sin(N_r\theta)] \\
\dot{i}_b &= \frac{1}{L}[v_b - Ri_b - K_m\omega \cos(N_r\theta)]
\end{aligned} \tag{1}$$

where v_a and v_b, and i_a and i_b are the voltages [V] and currents [A] of phases A and B, respectively. θ is the rotor (angular) position [rad], ω is the rotor (angular) velocity [rad/s], B is the viscous friction coefficient [N $\cdot$ m·s/rad], J is the inertia of the motor [Kg $\cdot$ m^2], K_m is the motor torque constant [N $\cdot$ m/A], R is the resistance of phase winding [Ω], L is the inductance of phase winding [H], and N_r is the number of rotor teeth. The load torque perturbation is denoted by τ_l. The derivative of the load torque τ_l with respect to time exists and is bounded, i.e., $\dot{\tau}_l = \delta_\tau$ is bounded, but unknown. Only position feedback is available and only the nominal value of $\frac{K_m}{JL}$ is known among PM stepper motor parameters. The model of the PM stepper motor (1) is 4^{th} order two-input single-output (TISO) system with the phases A and B voltage inputs and the position output.

B. Model Representation and Problem Formulation

The commutation scheme is defined as

$$\begin{aligned}
v_a &= -u\sin(N_r\theta) \\
v_b &= u\cos(N_r\theta)
\end{aligned} \tag{2}$$

where u is the control input for the new PM stepper motor model and has not yet been defined. The acceleration α and direct current i_d are defined as

$$\begin{aligned}
\alpha &= \dot{\omega} \\
&= \frac{1}{J}[-K_m i_a \sin(N_r\theta) + K_m i_b \cos(N_r\theta) - B\omega - \tau_l] \\
i_d &= i_a \cos(N_r\theta) + i_b \sin(N_r\theta).
\end{aligned} \tag{3}$$

We define the input gain, g, as

$$g = \frac{K_m}{JL} = g_0 + \Delta g \tag{4}$$

where g_0 is the nominal value of g and Δg represents the uncertainties in g. From (1), (2), and (3), the new SISO model of the PM stepper motor is obtained as

$$\begin{aligned}
\dot{z}_1 =& -\frac{1}{L}z_1 + \frac{N_r J}{K_m}x_2[\frac{B}{J}x_2 + x_3 + \tau_l] \\
\dot{x}_1 =& \, x_2 \\
\dot{x}_2 =& \, x_3 \\
\dot{x}_3 =& (g_0 + \Delta g)u - \frac{1}{JL}(BR + K_m^2 + N_r K_m L i_d)x_2 \\
& - \frac{JR + BL}{JL}x_3 - \frac{R}{JL}\tau_l - \frac{1}{J}\dot{\tau}_l
\end{aligned} \tag{5}$$

where $x_1 = \theta$, $x_2 = \omega$, $x_3 = \alpha$, and $z_1 = i_d$.

Remark 1: Generally $z_1 = i_d$ is controlled to a given reference, typically zero, in a permanent magnet synchronous motors (PMSMs) since the power consumption is a main issue. On the other hand, the control of i_d to be zero is not necessary since the PM stepper motors' power is small compared to the PMSMs [1]. In microstepping control widely used in the PM stepper motor, i_d is always positive [7]. In z_1 dynamics of model (5), if the second term $\frac{N_r J}{K_m}[\frac{B}{J}x_2 + x_3 + \tau_l]$ is bounded so that z_1 is input-to-state stable, then z_1 can be regarded as stable internal dynamics, and the SISO model of the PM stepper motor is thus a minimum phase nonlinear system. Consequently, only controls of x_1, x_2, and x_3 are needed for position control. In (5), x_1, x_2, and x_3 are controlled by the proposed control method.

In (5), the disturbance $d = x_4$ is defined as

$$\begin{aligned}
x_4 =& \, \Delta g u - \frac{1}{JL}(BR + K_m^2 + N_r K_m L i_d)x_2 \\
& - \frac{JR + BL}{JL}x_3 - \frac{R}{JL}\tau_l - \frac{1}{J}\dot{\tau}_l.
\end{aligned} \tag{6}$$

For the position control, PM stepper motor model (1) becomes a third order SISO system as

$$\begin{aligned}
\dot{z}_1 =& -\frac{1}{L}z_1 + \frac{N_r J}{K_m}x_2\left[\frac{B}{J}x_2 + x_3 + \tau_l\right] \\
\dot{x}_1 =& \, x_2 \\
\dot{x}_2 =& \, x_3 \\
\dot{x}_3 =& \, g_0 \, u + x_4
\end{aligned} \tag{7}$$

where $x = [x_1, \, x_2, \, x_3]^T$ is the state vector. The aim is to make the position x_1 track the desired position x_{1_d} using only position feedback and g_0 information. The desired position x_{1_d} is continuously differentiable up to the thirds order.

III. Nonlinear Gain Backstepping Controller

In this section, the design of the position tracking controller is discussed using a backstepping procedure. The tracking error $e = [e_1 \quad e_2 \quad e_3]^T$ is defined as

$$\begin{aligned}
e_1 =& \, x_1 - x_{1_d} \\
e_2 =& \, x_2 - x_{2_d} \\
e_3 =& \, x_3 - x_{3_d}
\end{aligned} \tag{8}$$

where x_{i_d}, $i \in [2, 3]$ has not yet been defined. From (7) and (8), the tracking error dynamics are written as

$$\begin{aligned}
\dot{e}_1 =& \, e_2 + x_{2_d} - \dot{x}_{1_d} \\
\dot{e}_2 =& \, e_3 + x_{3_d} - \dot{x}_{2_d} \\
\dot{e}_3 =& \, g_0 \, u + d - \dot{x}_{3_d}.
\end{aligned} \tag{9}$$

We define the desired state variable x_{i_d}, $i \in [2, 3]$ as

$$\begin{aligned}
x_{2_d} =& -k_1 e_1 + \dot{x}_{1_d} \\
x_{3_d} =& -k_2 e_2 + \dot{x}_{2_d}
\end{aligned} \tag{10}$$

where k_i, $i \in [1, 2]$ is a positive constant and a control gain.

From (9) and (10), the dynamics of e_i, $i \in [1, 2]$ become

$$\begin{aligned}
\dot{e}_1 =& -k_1 e_1 + e_2 \\
\dot{e}_2 =& -k_2 e_2 + e_3.
\end{aligned} \tag{11}$$

The control law u is designed as

$$\begin{aligned}
u =& \underbrace{\frac{1}{g_0}\left(-k_3 e_3 + \dot{x}_{3_d} - \hat{d}\right)}_{u_a} \\
& \underbrace{- \frac{1}{g_0}\left(k_{3_a}\sqrt{\hat{e}_1^2 + \nu_1} + k_{3_b}\sqrt{\hat{d}^2 + \nu_2}\right)e_3}_{u_b}
\end{aligned} \tag{12}$$

where k_3, k_{3_a}, k_{3_b}, ν_1, and ν_2 are positive constant and control gains, $\hat{e}_1 = \hat{x}_1 - x_{1_d}$ is the estimated position tracking error, and $\hat{x}_1$ and $\hat{d}$ are the estimated values of x_1 and d, respectively. The boundedness of $\hat{x}_1$ and $\hat{d}$ is guaranteed by the AOB that will be designed in Section IV.

Remark 2: In (12), the term u_a is used for stabilization, and u_b is a nonlinear gain term used to suppress the output tracking error when the disturbance estimation error increases. Since $d = f(x) + \Delta g(x)u + d_{ext}$, it may be difficult to estimate its exact value. Thus the disturbance estimation error may increase the position tracking error. The nonlinear gain is used to suppress the position tracking error when the position tracking error is increased due to the disturbance estimation error. As the disturbance estimation error increases, both the estimated position tracking error, $\hat{e}_1$, and the estimated disturbance, $\hat{d}$, may also increase. When $\hat{e}_1$ and $\hat{d}$ are large, the nonlinear gain term can enhance the damping effect. Note that the maximum value of the nonlinear gain can be chosen arbitrarily as k_{3_a} and k_{3_b}.

Using (12), we obtain the dynamics of e_3 as follows:

$$\dot{e}_3 = -k_3 e_3 - k_d\left(\hat{e}_1, \hat{d}\right)e_3 + d - \hat{d} \tag{13}$$

where $k_d(\hat{e}_1, \hat{d}) = k_{3_a}\sqrt{\hat{e}_1^2 + \nu_1} + k_{3_b}\sqrt{\hat{d}^2 + \nu_2}$. Now we study the stability of the dynamics of e_i, $i \in [1, 2]$ which can be written as follows:

$$\dot{e}_i = -k_i e_i + e_{i+1}. \tag{14}$$

At the next step, we assume that e_3 is ultimately bounded at the next step. We then obtain the dynamics of e_i^2 as

$$\begin{aligned}\frac{d}{dt}\left(\frac{e_i^2}{2}\right) &= -k_i e_i^2 + e_i e_{i+1} \\ &\leq -\frac{k_i}{2}e_i^2 - \frac{k_i}{2}|e_i|\left(|e_i| - \frac{2}{k_i}|e_{i+1}|\right). \end{aligned} \quad (15)$$

The following result is thus derived from (15), using Lemma 6.20 and Theorem C.2 in [25]:

$$|e_i(t)| \leq \exp\left(-\frac{k_i}{2}t\right)|e_i(0)| + \frac{2}{k_i}\sup_{0\leq\tau\leq t} e_{i+1}(\tau). \quad (16)$$

Equation (16) shows that the relationship between e_i and e_{i+1} has an ISS property. $\hat{d}$ is bounded by the AOB that will be designed in Section IV. The dynamics of e_3^2 are

$$\begin{aligned}\frac{d}{dt}\left(\frac{e_3^2}{2}\right) &= -k_3 e_3^2 - k_d\left(\hat{e}_1, \hat{d}\right)e_3^2 + (d-\hat{d})e_3 \\ &\leq -\frac{k_3}{2}e_3^2 - \left(\frac{k_3}{2} + k_d\left(\hat{e}_1, \hat{d}\right)\right)|e_3|(|e_3| - \sigma) \end{aligned} \quad (17)$$

where $\sigma = \frac{|d-\hat{d}|}{0.5k_3 + k_d(\hat{e}_1, \hat{d})}$. Then,

$$|e_3(t)| \leq \exp\left(-\frac{k_3}{2}t\right)|e_3(0)| + \frac{2}{k_3}\sup_{0\leq\tau\leq t}\sigma(\tau). \quad (18)$$

Equation (18) shows that the relationship between e_3 and σ has an ISS property. From (16) and (18), the ISS property of the overall tracking error system is

$$\begin{aligned}|e_1(t)| &\leq \exp\left(-\frac{k_1}{2}t\right)|e_1(0)| + \frac{2}{k_1}\sup_{0\leq\tau\leq t} e_2(\tau) \\ |e_2(t)| &\leq \exp\left(-\frac{k_2}{2}t\right)|e_2(0)| + \frac{2}{k_2}\sup_{0\leq\tau\leq t} e_3(\tau) \\ |e_3(t)| &\leq \exp\left(-\frac{k_3}{2}t\right)|e_3(0)| + \frac{2}{k_3}\sup_{0\leq\tau\leq t}\sigma(\tau). \end{aligned} \quad (19)$$

The overall tracking error system (19) is the serial interconnected system of the ISS system. We can thus conclude that the overall tracking error system (19) has an ISS property.

Remark 3: The upper bound of $|e_1|$ is determined by the constant control gainsk_1, k_2, k_3 and σ. As the values of $\hat{e}_1$ and $\hat{d}$ of $k_d(\hat{e}_1, \hat{d})$ in the denominator of σ increases, σ decreases: the nonlinear gain, $k_d(\hat{e}_1, \hat{d})$, in (12) grows so that the effects of $|d-\hat{d}|$ on $|e_1|$ can be sufficiently suppressed.

From (19), we obtain the following result:

$$\|e(t)\| \leq \sqrt{2}\alpha_3 \exp\left(-\frac{\kappa_3}{2}t\right)\|e(0)\| + \beta_3 \sup_{0\leq\tau\leq t}\sigma(\tau) \quad (20)$$

where $\alpha_1 = 1$, $\alpha_i = \alpha_{i-1}^2 + (\alpha_{i-1}+1)\beta_{i-1} + 1$, $i \in [2, n]$, $\beta_1 = \frac{2}{k_1}$, $\beta_i = ((\alpha_{i-1}+1)\beta_{i-1}+1)\frac{2}{k_i}$, $i \in [2,3]$, $\kappa_1 = k_1$, and $\kappa_i = \min(\frac{k_i}{2}, \frac{\kappa_{i-1}}{2})$, $i \in [2,3]$. Equation (20) guarantees the ISS of $\|e\|$. However, as the procedure for deriving (20) is lengthy and complicated, it is not included in this article.

We now consider the stability of the proposed controller. Suppose that the system state variables are constrained in a domain Ω_x. To guarantee that $x \in \Omega_x$, we need to guarantee that we can make $x \in D_x \subset \Omega_x$ where D_x is a compact set by the proposed controller. The desired output state vector x_d is defined as

$$x_d = \begin{bmatrix} x_{1_d} & \dot{x}_{1_d} & \ddot{x}_{1_d} \end{bmatrix}^T. \quad (21)$$

We design x_{1_d} such that $x_d \in \Omega_d \subset \Omega_x$ where Ω_d is a compact set. We define the compact set Ω_e as

$$\Omega_e = \{e | \|e\| \leq b_e\} \subset \mathbb{R}^3 \quad (22)$$

where b_e is a relatively small positive constant. If we choose sufficiently large control gains, an appropriate set of initial conditions to ensure $e \in \Omega_e$, given by, $e(0) \in \Omega_{e_0} \subset \Omega_e$ can be found. Ω_{e_0} is defined as

$$\Omega_{e_0} = \left\{e(0) | \sqrt{2}\alpha_3\|e(0)\| + \beta_3 \sup_{0\leq\tau\leq t}\sigma(\tau) \leq b_e\right\}. \quad (23)$$

As long as e is relatively small, x can track x_d with acceptable accuracy such that x does not escape from the domain of interest Ω_x. Consequently, since $e \in \Omega_e$ and $x_d \in \Omega_d$, it is guaranteed, from (8) and (10), that $x \in D_x \subset \Omega_x$.

Remark 4: To realize a small position tracking error, a very small value of b_e is not necessary; it is enough that b_e is chosen to be relatively smaller than $\|x_d\|$. From (19), we know that the position tracking error, e_1, can be sufficiently suppressed, even when b_e is not very small. Thus, a high control gain is not necessary for very small values of b_e. We also know from (19) that very small values of $|d-\hat{d}|$ are not required for precise position tracking. ◊

These results are summarized in the following Theorem.

Theorem 1: Consider the SISO PM stepper model (7) with the assumption that $\hat{e}_1$ and $\hat{d}$ are bounded. Suppose that $e(0) \in \Omega_{e_0} \subset \Omega_e$. If the controller defined as

$$\begin{aligned} x_{i_d} &= -k_{i-1}e_{i-1} + \dot{x}_{i-1_d},\ i \in [2,3] \\ u &= \frac{1}{g_0}\left(-k_3 e_3 + \dot{x}_{3_d} - \hat{d}\right) - \frac{1}{g_0}k_d\left(\hat{e}_1, \hat{d}\right)e_3 \end{aligned} \quad (24)$$

is implemented in the SISO PM stepper model (7), then the tracking error has the following properties.

1) A compact set D_x exists such that $x \in D_x \subset \Omega_x$.
2) ISS properties (19) and (20) are guaranteed.

◊

IV. Augmented Observer

The AOB is designed to estimate the full state and disturbance. We define the augmented state variable and its derivative as

$$\begin{aligned} x_4 &= d \\ \dot{x}_4 &= \delta. \end{aligned} \quad (25)$$

The estimated state, $\hat{x}$, and the augmented estimated state, $\hat{x}_a$, are defined as

$$\hat{x} = \begin{bmatrix}\hat{x}_1 & \hat{x}_2 & \hat{x}_3\end{bmatrix}^T,\ \hat{x}_a = \begin{bmatrix}\hat{x}_1 & \hat{x}_2 & \hat{x}_3 & \hat{x}_4\end{bmatrix}^T. \quad (26)$$

The AOB is designed as

$$\begin{aligned}\dot{\hat{x}}_1 &= \hat{x}_2 + \frac{l_1}{\varepsilon}(x_1 - \hat{x}_1)\\ \dot{\hat{x}}_2 &= \hat{x}_3 + \frac{l_2}{\varepsilon^2}(x_1 - \hat{x}_1)\\ \dot{\hat{x}}_3 &= \hat{x}_4 + g_0\, u + \frac{l_3}{\varepsilon^3}(x_1 - \hat{x}_1)\\ \dot{\hat{x}}_4 &= \frac{l_4}{\varepsilon^4}(x_1 - \hat{x}_1)\end{aligned} \tag{27}$$

where ε is a small positive constant and l_i, $i \in [1,4]$ is the observer gain. Note that ε is used to make the closed-loop system be in the form of the singular perturbed system [24]. The observer gain should be chosen such that the roots of the following are in the left-half plane

$$s^4 + l_1\, s^4 + l_2\, s^2 + l_3 s + l_4 = 0. \tag{28}$$

The estimation error $\tilde{x}$ and the augmented estimation error, $\tilde{x}_a$, are defined as

$$\tilde{x} = [\tilde{x}_1 \quad \tilde{x}_2 \quad \tilde{x}_3]^T,\ \tilde{x}_a = [\tilde{x}_1 \quad \tilde{x}_2 \quad \tilde{x}_3 \quad \tilde{x}_4]^T. \tag{29}$$

From (7), (25), (27), and (29), the augmented estimation error dynamics can be obtained as

$$\begin{aligned}\dot{\tilde{x}}_1 &= \tilde{x}_2 - \frac{l_1}{\varepsilon}\tilde{x}_1\\ \dot{\tilde{x}}_2 &= \tilde{x}_3 - \frac{l_2}{\varepsilon^2}\tilde{x}_1\\ \dot{\tilde{x}}_3 &= \tilde{x}_4 - \frac{l_3}{\varepsilon^3}\tilde{x}_1\\ \dot{\tilde{x}}_4 &= \delta - \frac{l_4}{\varepsilon^4}\tilde{x}_1.\end{aligned} \tag{30}$$

The scaled estimation error, $\eta = [\eta_1 \quad \eta_2 \quad \eta_3 \quad \eta_4]$, is defined as

$$\eta_1 = \frac{\tilde{x}_1}{\varepsilon^3},\ \eta_2 = \frac{\tilde{x}_2}{\varepsilon^2},\ \eta_3 = \frac{\tilde{x}_3}{\varepsilon},\ \eta_4 = \tilde{x}_4. \tag{31}$$

Thus, the scaled estimation error dynamics are

$$\varepsilon\dot{\eta} = A_\eta \eta + \varepsilon B_\eta \delta \tag{32}$$

where

$$A_\eta = \begin{bmatrix}-l_1 & 1 & 0 & 0\\ -l_2 & 0 & 1 & 0\\ -l_3 & 0 & 0 & 1\\ -l_4 & 0 & 0 & 0\end{bmatrix},\ B_\eta = \begin{bmatrix}0\\0\\0\\1\end{bmatrix}.$$

To choose an appropriate observer gain, the performance of the AOB in the frequency domain is studied. From (30), we obtain the transfer function $H(s) = \frac{\tilde{D}(s)}{D(s)}$ from d to $\tilde{d}$ as follows

$$H(s) := \frac{\varepsilon^4 s(s^3 + l_1\, s^2 + l_2\, s + l_3)}{s^4 + l_1\, s^3 + l_2\, s^2 + l_3 s + l_4} \tag{33}$$

where $D(s)$ and $\tilde{D}(s)$ are Laplace transforms of $d(t)$ and $\tilde{d}(t)$, respectively. As the transfer function $H(s)$ is in the form of a high pass filter, the cutoff frequency of $H(s)$ should be higher than the frequency of the main component in the disturbance. In (33), we see that the accuracy of state estimation depends on the bandwidth, of the AOB. However, in actual applications, the measurement noise may cause difficulties when using a wider bandwidth of AOB. Let us denote the measured output x_{1_m} as

$$x_{1_m} = x_1 + m \tag{34}$$

where m is the measurement noise. With a noisy measurement, the transfer function $H_m(s)$ from m to $\tilde{d}$ is obtained by

$$H_m(s) := \frac{\tilde{D}(s)}{M(s)} = \frac{(l_4 s^4 + l_3 s^2)}{s^4 + l_1\, s^3 + l_2\, s^2 + l_3 s + l_4} \tag{35}$$

where $M(s)$ is a Laplace transform of $m(t)$. From (35), the wider bandwidth of AOB may result in the amplification of the measurement noise.

Remark 5: From (33) and (35), the bandwidth of AOB should be chosen with consideration of a tradeoff between both estimation performance and amplification of the measurement noise. Fortunately, very small values of the estimation error, $\tilde{x}$, are not required for precise position tracking (as in Remark 4). Consequently, the need to increase the bandwidth of the AOB with the aim of reducing the disturbance estimation error can be avoided by nonlinear gain.

V. Closed-Loop Stability Analysis

As only output feedback is used, the estimated tracking error $\hat{e} = [\hat{e}_1 \quad \hat{e}_2 \quad \hat{e}_3]^T$ is defined as

$$\hat{e}_1 = \hat{x}_1 - x_{1_d}\hat{e}_2 = \hat{x}_2 - \hat{x}_{2_d}\hat{e}_3 = \hat{x}_3 - \hat{x}_{3_d} \tag{36}$$

where $\hat{x}_{i_d}$, $i \in [2,3]$ has not yet been defined. $\hat{x}$ in (24) is substituted for x, giving the following equation:

$$\begin{aligned}\hat{x}_{2_d} &= -k_1\hat{e}_1 + \dot{x}_{1_d}\\ \hat{x}_{3_d} &= -k_2\hat{e}_2 + \dot{\hat{x}}_{2_d}\\ \hat{u} &= \frac{1}{g_0}\left(-k_3\hat{e}_3 + \dot{\hat{x}}_{3_d} - \hat{x}_4\right) - \frac{1}{g_0}k_d\left(\hat{e}_1, \hat{d}\right)e_3.\end{aligned} \tag{37}$$

Note that the actual control input is not (24) but (37). To prove closed-loop stability, the control input is defined as $\hat{u}$. Equation (37) is implemented instead of (24) in (9). Thus, the tracking error dynamics are as follows:

$$\dot{e} = A_e e + B_e \xi \tag{38}$$

where

$$A_e = \begin{bmatrix}-k_1 & 1 & 0\\ 0 & -k_2 & 1\\ 0 & 0 & -k_3\end{bmatrix},\ B_e = \begin{bmatrix}0\\0\\1\end{bmatrix}$$

$$\xi = g_0(\hat{u} - u) - k_d\left(\hat{e}_1, \hat{d}\right)e_3 + d - \hat{d}.$$

The closed-loop system is formulated using (32) and (38) as

$$\begin{aligned}\dot{e} &= A_e e + B_e \xi\\ \varepsilon\dot{\eta} &= A_\eta \eta + \varepsilon B_\eta \delta.\end{aligned} \tag{39}$$

Equation (39) is in the form of a singular perturbation system. The dynamics of e are slow, and the dynamics of η are fast. A short transient period exists, during which the fast states, η, decay to the $O(\varepsilon)$ level, while the slow states, e, remain

within Ω_e. First, we consider the behavior of the slow system. Using a similar process to that described in Section III, an appropriate estimate for the slow system can be found, such that $e(0) \in \Omega_{e_0\varepsilon} \subset \Omega_e$, where $\Omega_{e_0\varepsilon}$ is yet to be defined. Since A_η is a Hurwitz matrix, a positive constant, b_ξ, exists, such that $\|B_e\xi\| \le b_\xi$, as long as $e \in \Omega_e$. The Lyapunov candidate function, V_e, is defined as

$$V_e = e^T P_e e \tag{40}$$

where $P_e \succ 0$ is the solution of $A_e P_e + P_e A_e^T = -Q_e$ such that $Q_e \succ 0$. The derivative of V_e with respect to time is given by

$$\begin{aligned}\dot{V}_e =& -e^T Q_e e + 2e^T P_e B_e \xi \\ \le& -e^T Q_e e + 2b_\xi \|P_e\|\|e\| \\ \le& -2\gamma_e V_e + 2\mu_e \sqrt{V_e}\end{aligned} \tag{41}$$

where $\gamma_e = \frac{\lambda_{\min}(Q_e)}{2\lambda_{\max}(P_e)}$, $\mu_e = \frac{b_\xi \|P_e\|}{\sqrt{\lambda_{\min}(P_e)}}$, and $\lambda_{\min}(P_e)$ and $\lambda_{\max}(P_e)$ are the respective minimum and maximum eigenvalues of P_e. From (41), we obtain

$$\sqrt{V_e(t)} \le \exp(-\gamma_e t)\sqrt{V_e(0)} + \frac{\mu_e}{\gamma_e}(1 - \exp(-\gamma_e t)). \tag{42}$$

Since $\sqrt{\lambda_{\min}(P_e)}\|e\| \le \sqrt{V_e} \le \sqrt{\lambda_{\max}(P_e)}\|e\|$,

$$\begin{aligned}\|e(t)\| \le& \sqrt{\frac{\lambda_{\max}(P_e)}{\lambda_{\min}(P_e)}} \exp(-\gamma_e t)\|e(0)\| \\ &+ \frac{\mu_e}{\gamma_e \sqrt{\lambda_{\min}(P_e)}}(1 - \exp(-\gamma_e t)).\end{aligned} \tag{43}$$

If the initial conditions are selected such that for some positive constant, b_{e_0}, $\|e(0)\| \le b_{e_0} < b_e$, a time T_2 exists such that over the time interval, $[0,\ T_2)$, $e \in \Omega_e$ regardless of ε.

Assumption 1: The rate of change of the disturbance d_{ext} exists and is bounded, i.e., $\dot{d}_{ext}$ is bounded but unknown. ♢

From Assumption 1, $\dot{d} = \delta$ is bounded over the time interval $[0,\ T_2)$. Thus a positive constant $\delta_{\max}$ exists such that $|\dot{d}| = |\delta| \le \delta_{\max}$. We define the Lyapunov candidate function V_η as

$$V_\eta = \eta^T P_\eta \eta \tag{44}$$

where $P_\eta \succ 0$ is the solution of $A_\eta P_\eta + P_\eta A_\eta^T = -Q_\eta$ for $Q_\eta \succ 0$. We obtain $\dot{V}_\eta$ as

$$\begin{aligned}\dot{V}_\eta =& -\frac{1}{\varepsilon}\eta^T Q_\eta \eta + 2\eta^T P_\eta B_\eta \delta \\ \le& -\frac{1}{\varepsilon}\eta^T Q_\eta \eta + 2\delta_{\max}\|P_\eta B_\eta\|\|\eta\| \\ \le& -\frac{2\gamma_\eta}{\varepsilon}V_\eta + \mu_\eta\sqrt{V_\eta} = -\frac{\gamma_\eta}{\varepsilon}V_\eta - \frac{\gamma_\eta}{\varepsilon}V_\eta + \mu_\eta\sqrt{V_\eta}\end{aligned} \tag{45}$$

where $\gamma_\eta = \frac{\lambda_{\min}(Q_\eta)}{2\lambda_{\max}(P_\eta)}$, $\mu_\eta = \frac{2\delta_{\max}\|P_\eta B_\eta\|}{\sqrt{\lambda_{\min}(P_\eta)}}$. If $V_\eta \ge \varepsilon^2\rho_\eta$ where $\rho_\eta = (\frac{\mu_\eta}{\gamma_\eta})^2$, (45) becomes

$$\dot{V}_\eta \le -\frac{\gamma_\eta}{\varepsilon}V_\eta. \tag{46}$$

Equation (31) indicates that $V_\eta(0) = \eta^T(0)P_\eta\eta(0)$ is bounded by $\frac{b_{\eta_0}}{\varepsilon^6}$ for some positive b_{η_0}. As long as $V_\eta \ge \varepsilon^2\rho_\eta$ over the time interval $[0,\ T_2)$, the following relations hold

$$V_\eta \le \exp\left(-\frac{\gamma_\eta}{\varepsilon}t\right)V_\eta(0) \le \frac{b_{\eta_0}}{\varepsilon^6}\exp\left(-\frac{\gamma_\eta}{\varepsilon}t\right). \tag{47}$$

Thus, the time $T_1(\varepsilon)$ when $V_\eta = \varepsilon^2\rho_\eta$ can be obtained as

$$T_1 = \frac{\varepsilon}{\gamma_\eta}\ln\left(\frac{b_{\eta_0}}{\rho_\eta\varepsilon^8}\right). \tag{48}$$

From (48), we see that the time when $V_\eta = \varepsilon^2\rho_\eta$, depends on ε. $T_1(\varepsilon)$ tends to zero, as ε tends to ∞, $T_1(\varepsilon)$ goes to zero. Thus, ε^* exists, such that for $\varepsilon \in (0,\ \varepsilon^*]$, $T_1 \in (0,\ \frac{T_2}{2})$. $V_\eta(t) \le \rho_\eta\varepsilon^2$ for all values in the interval, $t \in [T_1, T_3]$, where e escapes from the set Ω_e for the first time in T_3. An explanation for why T_3 can be extended to ∞ is provided later in this section.

We studied the behavior of the slow system, e, over the time interval $[T_1,\ T_3)$. Over this time interval, as $V_\eta(t) \le \rho_\eta\varepsilon^2$, η is of the order $O(\varepsilon)$. Because the control input, u, which uses the estimation states, $\hat{x}$, is applied to the third subsystem of the slow system e, the behavior of the third subsystem can be studied using the cascade characteristics defined in the backstepping design procedure. In u (24) and $\hat{u}$ (37), the different desired states, x_{i_d} and $\hat{x}_{i_d}$ $i \in [2, 3]$, are used, respectively. In contrast, x_{1_d} is used in both u (24) and $\hat{u}$ (37). Thus, there exists $k_{\tilde{x}} > 0$ [26] such that

$$|\hat{u}(\hat{x}, x_{1_d}) - u(x, x_{1_d})| \le k_{\tilde{x}}\|\hat{x} - x\|. \tag{49}$$

Since η is of $O(\varepsilon)$, we have

$$|\hat{u}(\hat{x}, x_{1_d}) - u(x, x_{1_d})| \le k_\varepsilon \varepsilon \tag{50}$$

where $k_\varepsilon > 0$. Since $\hat{u}$ (37) is substituted for u (24) the dynamics of e_3, (13) becomes

$$\dot{e}_3 = -k_3 e_3 - k_d\left(\hat{e}_1, \hat{d}\right)e_3 + d - \hat{d} + g_0(\hat{u}(\hat{x}, x_1^d) - u(x, x_1^d)). \tag{51}$$

Equation (17) also changes into

$$\frac{d}{dt}\left(\frac{e_3^2}{2}\right) \le -\frac{k_3}{2}e_3^2 + \left(\frac{k_3}{2} + k_d\left(\hat{e}_1, \hat{d}\right)\right)|e_3|(|e_3| - \sigma_\varepsilon) \tag{52}$$

where $\sigma_\varepsilon = \frac{|d-\hat{d}| + g_0(\hat{u}(\hat{x}, x_1^d) - u(x, x_1^d))}{0.5k_3 + k_d(\hat{e}_1, \hat{d})}$. From (50)

$$\sigma_\varepsilon = \frac{|d - \hat{d}| + g_0(\hat{u}(\hat{x}, x_1^d) - u(x, x_1^d))}{0.5k_3 + k_d\left(\hat{e}_1, \hat{d}\right)} \le \sigma + k_{e_3}\varepsilon \tag{53}$$

for some $k_{e_3} > 0$. The behavior of e for $t \in [0,\ T_1)$ is characterized in (43). The following considers the behavior of e when the starting time is T_1, i.e., $t \in [T_1,\ T_3)$. Equation (18) is rewritten as

$$\begin{aligned}|e_3(t)| \le& \exp\left(-\frac{k_3}{2}(t - T_1)\right)|e_3(T_1)| \\ &+ \frac{2}{k_3}\sup_{T_1 \le \tau \le t}\sigma(\tau) + k_{e_3}\varepsilon.\end{aligned} \tag{54}$$

For any $\varepsilon \in (0,\ \varepsilon^*]$ (54) shows the input-to-state practical stability (ISpS), which is an extension of the concept of the ISS

property of e_3 dynamics [27]. Finally

$$\|e(t)\| \leq \sqrt{2}\alpha_3 \exp\left(-\frac{k_3}{2}(t-T_1)\right)\|e(T_1)\| + \beta_3 \sup_{T_1\leq\tau\leq t}\sigma(\tau) + k_e\varepsilon \quad (55)$$

for some $k_e > 0$. Similar to Ω_{e_0} defined in (23), an appropriate set of initial conditions $e(0) \in \Omega_{e_0\varepsilon} \subset \Omega_e$ can be found according to (43) and (55) as

$$\Omega_{e_0\varepsilon} = \{e(0)|\|e(0)\| \leq b_{e_0} < b_e, \sqrt{2}\alpha_3\|e(T_1)\| + \beta_3 \sup_{T_1\leq\tau\leq t}\sigma(\tau) + k_e\varepsilon \leq b_e\}. \quad (56)$$

In (56), $\|e(T_1)\|$ can be obtained as follows:

$$\|e(T_1)\| \leq \sqrt{\frac{\lambda_{\max}(P_e)}{\lambda_{\min}(P_e)}}\exp(-\gamma_e T_1)\|e(0)\| + \frac{\mu_e}{\gamma_e\sqrt{\lambda_{\min}(P_e)}}(1-\exp(-\gamma_e T_1)). \quad (57)$$

Thus, using (56) and (57), we can make $e \in \Omega_e$ provided a sufficiently small interval, $\varepsilon \in (0,\ \varepsilon^*]$, exist. Consequently, we can consider that the escape time T_3 becomes ∞. The performance of the proposed method (27) and (37) is summarized in the following Theorem.

Theorem 2: Consider the SISO PM stepper motor model (7). Under Assumption 1, we suppose that $e(0) \in \Omega_{e_0\varepsilon} \subset \Omega_e$. If the proposed method (27) and (37) is implemented in the SISO PM stepper motor model (7), then there exists ε^* such that for all $\varepsilon \in (0, \varepsilon^*]$, the ISpS properties of the tracking error system are guaranteed by

$$|e_1(t)| \leq \exp\left(-\frac{k_1}{2}t\right)|e_1(0)| + \frac{2}{k_1}\sup_{0\leq\tau\leq t}e_2(\tau)$$

$$|e_2(t)| \leq \exp\left(-\frac{k_2}{2}t\right)|e_2(0)| + \frac{2}{k_2}\sup_{0\leq\tau\leq t}e_3(\tau)$$

$$|e_3(t)| \leq \exp\left(-\frac{k_3}{2}(t-T_1)\right)|e_3(T_1)| + \frac{2}{k_3}\sup_{T_1\leq\tau\leq t}\sigma(\tau) + k_{e_3}\varepsilon \quad (58)$$

and

$$\|e(t)\| \leq \sqrt{2}\alpha_3 \exp\left(-\frac{k_3}{2}(t-T_1)\right)\|e(T_1)\| + \beta_3 \sup_{T_1\leq\tau\leq t}\sigma(\tau) + k_e\varepsilon. \quad (59)$$

Remark 6: Note that $T_1(\varepsilon) \to 0$ as $\varepsilon \to 0$. Therefore, as long as ε is close to zero, the properties of the tracking error with the output feedback can be recovered. In addition, the properties of the tracking error with output feedback, (58) and (59), are closer to those of full-state feedback, (19) and (20).

Remark 7: From (58), it is evident that the tracking error system in (38) is also the serial interconnected system of the ISS system. Thus, the output tracking error, e_1 can be sufficient, even suppressed though the estimation error is not very small. This means that a very small estimation error, $\tilde{x}$, is not required to realize precise output tracking. ◊

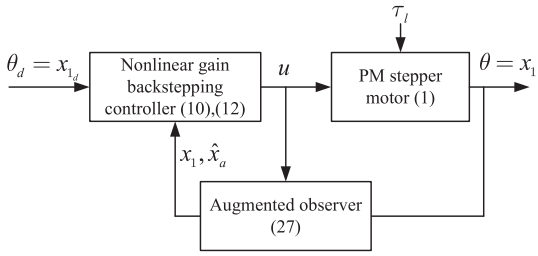

Fig. 1. Block diagram of the proposed method.

The block diagram of the proposed method is shown is Fig. 1. The augmented observer (27) estimates x_a using the feedback of x_1. Then, the nonlinear gain backstepping controller (10) and (12) generates the control input u using $\hat{x}_a$ and x_1. Now, we provide the gain tuning guideline for the controller (10), (12) and observer (27). The gains for the controller (10), (12), and observer (27) can be tuned as follows:

1) *Step 1 - Observer Gain:* To decide observer gains of the AOB, it is important to determine the cutoff frequency of the transfer function $H(s) = \frac{\tilde{D}(s)}{D(s)}$. The observer gains l_1, l_2, l_3, and l_4 are determined such that the cutoff frequency of the transfer function $H(s) = \frac{\tilde{D}(s)}{D(s)}$ is higher than the expected frequency of the disturbance.
2) *Step 2 - Controller Gain for u_a:* The proposed controller consists of the stabilization part u_a and the nonlinear gain part u_b. For the stabilization, the k_1 and k_2 for u_a are tuned without the use of u_b, first. The control gain k_1 for the position tracking error e_1 is determined to be relatively larger than k_2 and k_3 because the control objective is the position tracking as follows: $k_1 \geq 10k_2$ and $k_2 \geq k_3 \quad \forall k_1, k_2, k_3 > 0$.
3) *Step 3 - Controller Gain for u_b:* The nonlinear gain part u_b is used to suppress the position tracking error when the position tracking and the disturbance increases. ν_1, k_{3a}, ν_2, and k_{3b} are determined to be relatively much smaller than k_2 and k_3 to avoid the input saturation as follows: (1) $k_3 > 100k_{3a}$ and $k_3 > 100k_{3b}$ and (2) $\nu_1 > 10k_{3a}$ and $\nu_2 > 10k_{3b}$.

VI. Simulations and Experiments

The performance of the proposed method was evaluated via simulations and experiments. The parameters of the PM stepper motor are $L = 0.0144$ H, $R = 4.5\ \Omega$, $J = 3 \times 10^{-5}$ Kg ·m^2, $K_m = 0.88$ N · m/A, $N_r = 50$, and $B = 1 \times 10^{-4}$ N · m·s/rad. To validate the robustness performance of the proposed method, only position feedback and nominal value of $\frac{K_m}{JL}$ among all parameters of the PM stepper motor were used. The used control and observer gains are as follows: $k_1 = 3000$, $k_2 = 100$, $k_3 = 100$, $k_{3_a} = 0.01, \nu_1 = 1, k_{3_b} = 0.01, \nu_2 = 1, l_1 = 2.011 \times 10^3$, $l_2 = 1.516 \times 10^6$, $l_3 = 5.080 \times 10^8$, and $l_4 = 6.3838 \times 10^{10}$.

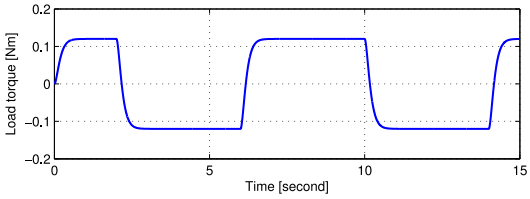

Fig. 2. Load torque, τ_l.

A. Simulation Results

In simulations, to evaluate the performance of the proposed method, the proposed method was compared to the backstepping controller [25] as follows:

$$\begin{aligned}\hat{x}_{2_d} &= -k_1\hat{e}_1 + \dot{x}_{1_d}\\ \hat{x}_{3_d} &= -k_2\hat{e}_2 + \dot{\hat{x}}_{2_d}\\ \hat{u} &= \frac{1}{g_0}\left(-k_3\hat{e}_3 + \dot{\hat{x}}_{3_d} - \hat{x}_4\right)\end{aligned} \tag{60}$$

where $k_1 = 3000$, $k_2 = 100$, $k_3 = 400$, $k_{3_a} = 0$, $\nu_1 = 1$, $k_{3_b} = 0$, $\nu_2 = 1$. In the backstepping controller (60), the AOB (27) with the same observer gain was used. The desired position, $\theta_d = (1 + e^{-20t})\pi \sin(0.25\pi t)$ was used. The load torque, τ_l, was used as shown in Fig. 2.

The estimation performance for the proposed method is shown in Fig. 3. The peaking of velocity at the desired position resulted in the appearance of peaking phenomena for the estimated acceleration and disturbance. In addition, acceleration was estimated well, during peaking at the initial time. However, the estimated disturbance did not make a perfect track of the actual disturbance, because the peaking speed exceeded the bandwidth of the observer. It is inferred that these peaking phenomena were caused by the initial desired velocity and not by the observer gain. The position tracking errors for both methods are shown in Fig. 4. The peaking phenomena observed with state estimation, caused the position tracking error peaking phenomenon at the initial position in the backstepping controller However, the nonlinear gain suppressed the position tracking error peaking phenomenon in the proposed method. Furthermore, the magnitude of the position tracking error was reduced by applying nonlinear gain in the steady-state response.

B. Experimental Results

Experiments were performed by utilizing a PM stepper motor driver set to validate the performance of the proposed method. Fig. 5 shows the hardware configuration of the motor driver set. Experiments were performed using ControlDesk software, two RapidPro, and a SCALEXIO real-time system. We generated a real-time control code in Matlab/Simulink to apply ControlDesk. SCALEXIO supported a maximum sample rate of 40 kHz. Each RapidPro unit consisted of three half-bridge power stage modules. The two switches of each half bridge were driven by complementary signals with dead time to prevent feed-through faults. The PM stepper motor (57HS41-1004, NEMA & Co) was directly connected to an encoder (2500 pulses per revolution). A shaft brake manufactured by Mobac Co. (FAT 20 RR), was

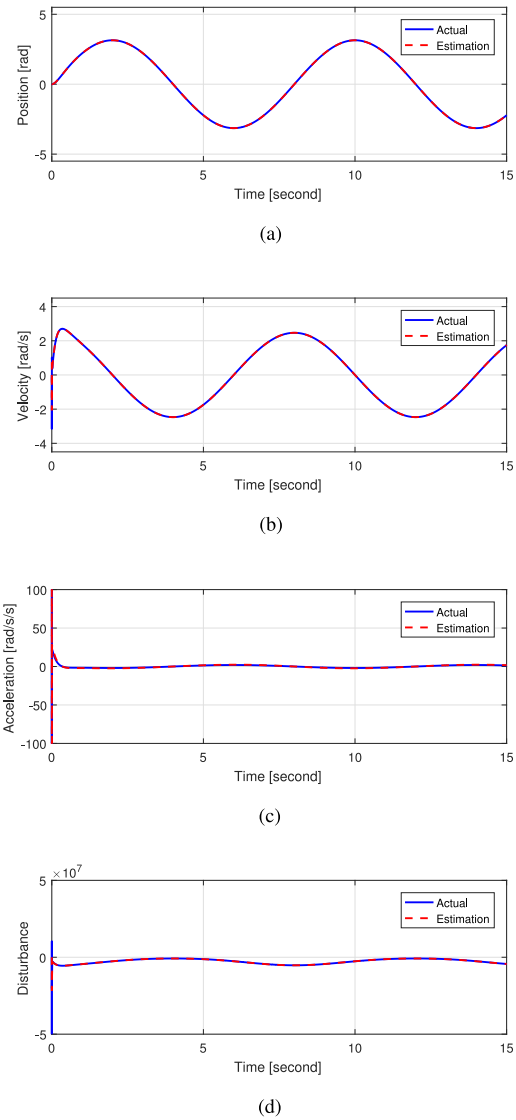

Fig. 3. Estimation performance for the proposed method in simulations. (a) Position, θ. (b) Velocity, ω. (c) Acceleration, α. (d) Disturbance, d.

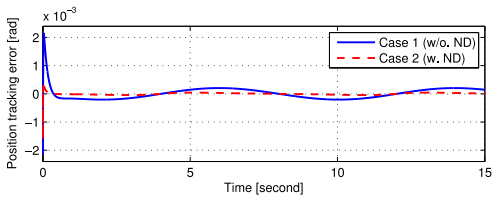

Fig. 4. Position tracking errors, $\theta_d - \theta$ of the backstepping controller and the proposed method in simulations.

used to generate the load torque. A personal computer was used to implement the control program in C language, compile the program, and upload executable output code to the SCALEXIO real-time system. The switching frequency was set to be 20 kHz to evaluate the performance of the proposed method for low frequency inverters.

In experiments, to evaluate the performance of the proposed method, the proposed method was compared to the backstepping controller (60) and the proportional-integral (PI) controller as

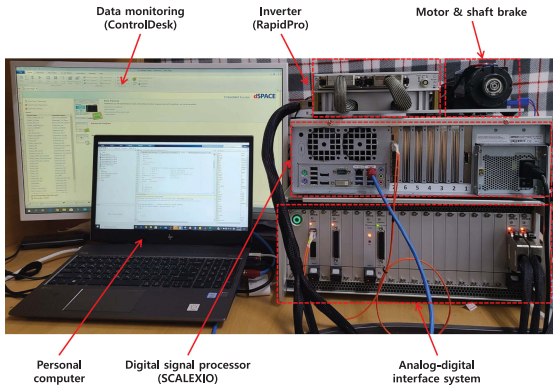

Fig. 5. Hardware configuration for the experiments.

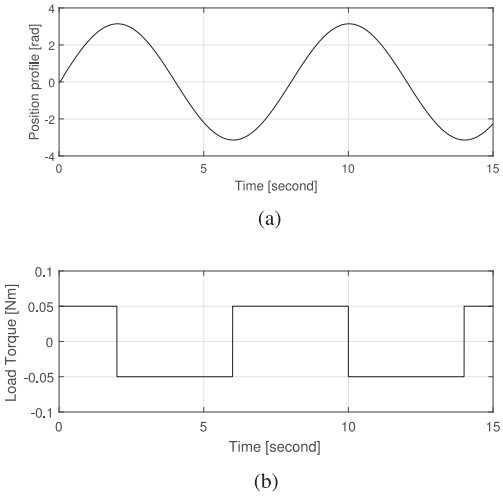

Fig. 6. Slow desired position $\theta_d = 3\sin(0.25 \times 2\pi t)$ and the load torque in experiments. (a) Desired position. (b) Load torque, τ_l.

follows:

$$\begin{aligned}
\tau_d &= k_P(\theta_d - \theta) + k_I \int_0^t (\theta_d - \theta)d\tau + k_D(\dot{\theta}_d - \dot{\theta}) \\
&\quad + B\omega_d + J\dot{\omega}_d \\
i_{a_d} &= -\frac{\tau_d}{K_m}\sin(N_r\theta) \\
i_{b_d} &= \frac{\tau_d}{K_m}\cos(N_r\theta) \\
v_a &= k_{pi}(i_{a_d} - i_a) + k_{Ii}\int_0^t (i_{a_d} - i_a)d\tau + k_{Di}(i_{a_d} - i_a) \\
v_b &= k_{pi}(i_{b_d} - i_b) + k_{Ii}\int_0^t (i_{b_d} - i_b)d\tau + k_{Di}(i_{b_d} - i_b)
\end{aligned} \tag{61}$$

where $k_P = 4000$, $k_I = 10$, $k_D = 130$, $k_{pi} = 1000$, $k_{Ii} = 20$, and $k_{Di} = 200$. Two desired positions were used as follows: The slow desired position $\theta_d = (1 + e^{-20t})\pi\sin(0.25\pi t)$ and the fast desired position $\theta_d = (1 + e^{-20t})\pi\sin(2\pi t)$.

The slow desired position $\theta_d = (1 + e^{-20t})\pi\sin(0.25\pi t)$ and the load torque were used as shown in Fig. 6. The

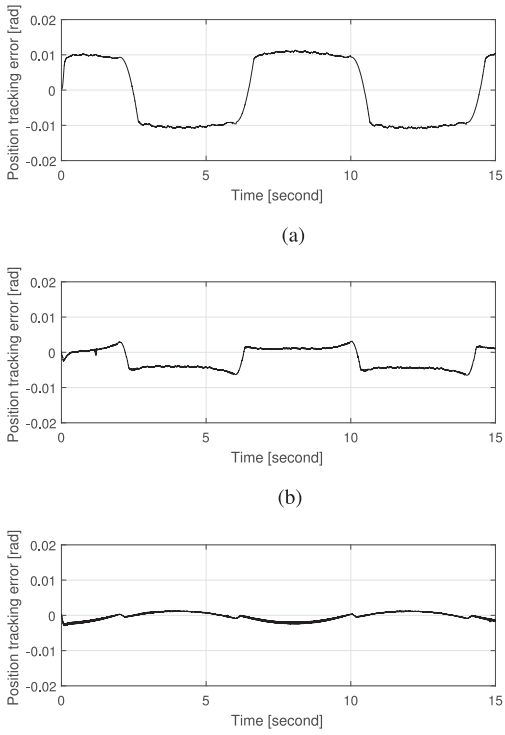

Fig. 7. Position tracking errors of three methods with the slow desired position $\theta_d = 3\sin(0.25 \times 2\pi t)$ in experiments. (a) PI controller. (b) Backstepping. (c) Proposed method.

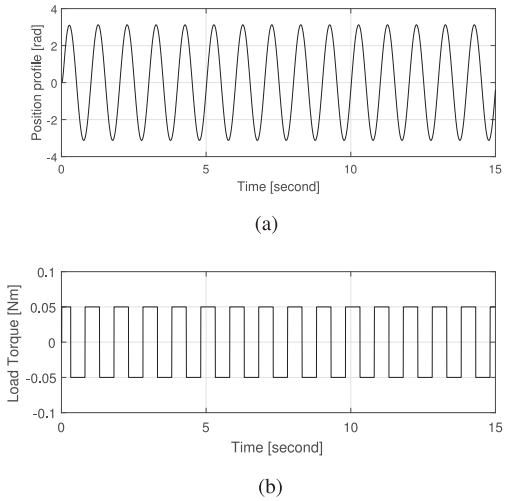

Fig. 8. Fast desired position $\theta_d = 3\sin(2\pi t)$ and the load torque in experiments. (a) Desired position. (b) Load torque, τ_l.

position tracking errors of three methods with the slow desired position are shown in Fig. 7. When the velocity changed, the load torque changed according to the velocity. Furthermore, Coulomb friction existed. Thus, it was difficult to accurately estimate disturbance without the high observer gain unlike the simulations Consequently, the position tracking errors increased during velocity change although the estimated disturbances were compensated for. The backstepping controller (60) and the

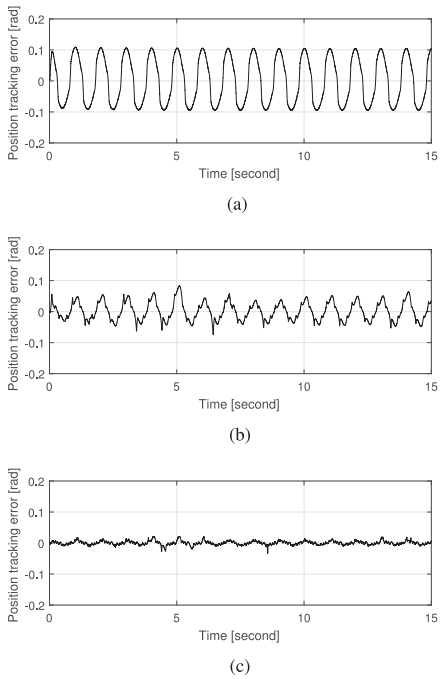

Fig. 9. Position tracking errors of three methods with the fast desired position $\theta_d = 3\sin(2\pi t)$ in experiments. (a) PID controller. (b) Backstepping. (c) Proposed method.

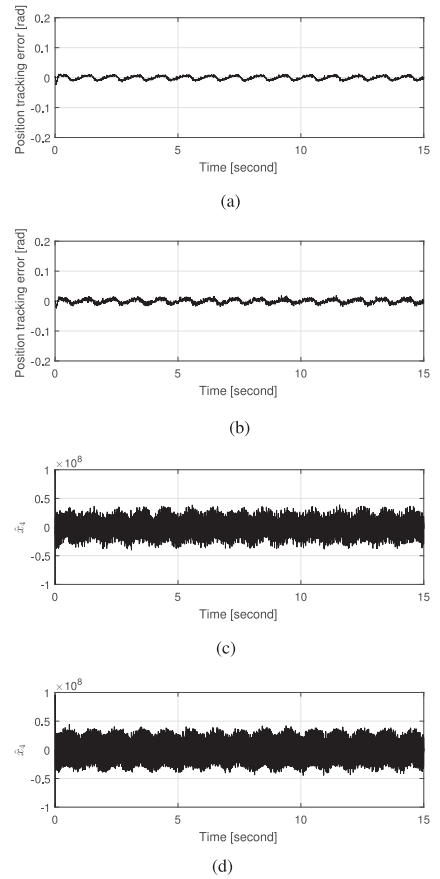

Fig. 10. Position tracking errors and estimated disturbances of the proposed method for Cases 1 and 2. (a) Position tracking error for Case 1. (b) Position tracking error for Case 2. (c) Estimated disturbance for Case 1. (d) Estimated disturbance for Case 2.

PI controller (61) had a relatively large position tracking error. On the other hand, in the proposed method, the position tracking error was suppressed by the increased nonlinear gain according to the increased the position tracking error and the increased estimated disturbance. Thus, the position tracking error of the proposed method was the smallest among the three methods.

The fast desired position $\theta_d = (1 + e^{-20t})\pi \sin(2\pi t)$ and the load torque were used as shown in Fig. 8. The position tracking errors of three methods with the fast desired position are shown in Fig. 9. Like the experimental result with the slow desired position, the proposed method had the smallest position tracking error among three methods. To evaluate the robustness performance of the proposed method, the experiments were conducted with the uncertainty for g_0. Two cases were tested as follows: (1) Case 1: the proposed method without the uncertainty for g_0; and (2) Case 2: the proposed method with the uncertainty (50 %) for g_0. The fast desired position $\theta_d = 3\sin(2\pi t)$ was used. Fig. 10 shows the position tracking errors and the estimated disturbances inputs of the proposed method for Cases 1 and 2. The amplitude of the position tracking error for Case 1 was similar to that of the position tracking error for Case 2 because the proposed method has the robustness against the uncertainty for g_0. In Case 2, the uncertainty (50 %) for g_0 exists, thus this uncertainty was included in the disturbance x_4. Consequently, the estimated disturbance $\hat{x}_4$ also included the uncertainty (50 %) for g_0 so the amplitude of $\hat{x}_4$ for Case 2 was larger than that for Case 1.

VII. Conclusion

In this article, nonlinear gain backstepping control with AOB was developed to enable position control of PM stepper motors. The SISO model comprising position, velocity, and acceleration was developed using a commutation scheme to enable position control of the PM stepper motor. External disturbances, acceleration dynamics, and parameter uncertainties were all considered as disturbances. The AOB was designed to estimate the full state and disturbance, and a nonlinear controller was then developed to suppress the increase in position tracking errors while enabling an increase in the estimation error of the disturbance. The performance of the proposed method was subsequently validated via simulations and experiments, in which the position tracking error in the transient response was reduced by nonlinear gain.

References

[1] T. Kenjo, *Stepping Motors and Their Microprocessor Control*. Oxford, U.K.: Clarendon, 1984.

[2] A. Ariasa, J. Caum, and R. Griñóa, "Moving towards the maximum speed in stepping motors by means of enlarging the bandwidth of the current controller," *Mechatronics*, vol. 40, pp. 51–62, 2016.

[3] D. Shin, W. Kim, Y. Lee, and C. C. Chung, "Phase compensated microstepping for permanent magnet stepper motors," *IEEE Trans. Ind. Electron.*, vol. 60, no. 12, pp. 5773–5780, Dec. 2013.

[4] M. Bodson, J. Chiasson, R. Novotnak, and R. Rekowski, "High-performance nonlinear feedback control of a permanent magnet stepper motor," *IEEE Trans. Control Syst. Technol.*, vol. 1, no. 1, pp. 5–14, Mar. 1993.

[5] J.-J. Chen and K.-P. Chin, "Automatic flux-weakening control of permanent magnet synchronous motors using a reduced-order controller," *IEEE Trans. Power Electron.*, vol. 15, no. 5, pp. 881–890, Sep. 2000.
[6] J. Lee, J. Hong, K. Nam, R. Ortega, L. Praly,, and A. Astolfi, "Sensorless control of surface-mount permanent-magnet synchronous motors based on a nonlinear observer," *IEEE Trans. Power Electron.*, vol. 25, no. 2, pp. 290–297, Feb. 2010.
[7] W. Kim, D. Shin, and C. C. Chung, "Microstepping with nonlinear torque modulation for permanent magnet stepper motors," *IEEE Trans. Control Syst. Technol.*, vol. 21, no. 5, pp. 1971–1979, Sep. 2013.
[8] D. Shin, W. Kim, Y. Lee, and C. C. Chung, "Nonlinear control with state-dependent reset integrator for a class of singularly perturbed interconnected nonlinear systems," *IEEE Trans. Control Syst. Technol.*, vol. 25, no. 4, pp. 1193–1203, Jul. 2017.
[9] D. Shin, W. Kim, Y. Lee, and C. C. Chung, "Enhanced nonlinear damping for a class of singularly perturbed interconnected nonlinear systems," *Automatica*, vol. 65, no. 1, pp. 36–42, 2016.
[10] Y. Lee, D. Shin, W. Kim, and C. C. Chung, "Nonlinear $\mathcal{H}_2$ control for a nonlinear system with bounded varying parameters: Application to PM stepper motors," *IEEE/ASME Trans. Mechatronics*, vol. 22, no. 3, pp. 1349–1359, Jun. 2017.
[11] K. M. Le, H. V. Hoang, and J. W. Jeon, "An advanced closed-loop control to improve the performance of hybrid stepper motors," *IEEE Trans. Power Electron.*, vol. 32, no. 9, pp. 7244–7255, Sep. 2017.
[12] Z. Zhou, C. Xia, Y. Yan, Z. Wang, and T. Shi, "Disturbances attenuation of permanent magnet synchronous motor drives using cascaded predictive-integral-resonant controllers," *IEEE Trans. Power Electron.*, vol. 33, no. 2, pp. 1514–1527, Feb. 2018.
[13] Y. Lee, J. Gil, and W. Kim, "Velocity control for sideband harmonics compensation in permanent magnet synchronous motors with low switching frequency inverter," *IEEE Trans. Ind. Electron*, vol. 68, no. 4, pp. 3434–3444, Apr. 2021.
[14] A. J. Blauch, M. Bodson, and J. Chiasson, "High-speed parameter estimation of stepper motors," *IEEE Trans. Control Syst. Technol.*, vol. 1, no. 4, pp. 270–279, Dec. 1993.
[15] S. Kim, K. Lee, and K. Lee, "Singularity-free adaptive speed tracking control for uncertain permanent magnet synchronous motor," *IEEE Trans. Power Electron.*, vol. 31, no. 2, pp. 1692–1701, Feb. 2016.
[16] S.-K. Kim, J.-S. Lee, and K.-B. Lee, "Offset-free robust adaptive backstepping speed control for uncertain permanent magnet synchronous motor," *IEEE Trans. Power Electron.*, vol. 31, no. 10, pp. 7065–7076, Oct. 2016.
[17] P. Krishnamurthy and F. Khorrami, "Voltage-fed permanent-magnet stepper motor control via position-only feedback," *IEE Proc.-Control Theory Appl.*, vol. 151, no. 4, pp. 499–510, Jul. 2004.
[18] M. Defoort, F. Nollet, T. Floquet, and W. Perruquetti, "A third-order sliding-mode controller for a stepper motor," *IEEE Trans. Ind. Electron.*, vol. 56, no. 9, pp. 3337–3336, Sep. 2009.
[19] H. Du, G. Wen, Y. Cheng,, and J. Lu, "Design and implementation of bounded finite-time control algorithm for speed regulation of permanent magnet synchronous motor," IEEE Trans. Ind. Electron, vol. 68, no. 3, pp. 2417–2426, Mar. 2021.
[20] J. Han, "From PID to active disturbance rejection control," *IEEE Trans. Ind. Electron.*, vol. 56, no. 3, pp. 900–906, Mar. 2009.
[21] Q. Guo, Y. Zhang, B. G. Celler, and S. W. Su, "Backstepping control of electro-hydraulic system based on extended-state-observer with plant dynamics largely unknown," *IEEE Trans. Ind. Electron.*, vol. 63, no. 11, pp. 6909–6920, Nov. 2016.
[22] X. Zhang, and Z. Li, "Sliding-mode observer-based mechanical parameter estimation for permanent magnet synchronous motor," *IEEE Trans. Power Electron.*, vol. 31, no. 8, pp. 5732–5745, Aug. 2016.
[23] D. Zheng and H. Xu, "Adaptive backstepping-flatness control based on an adaptive state observer for a torque tracking electrohydraulic system," *IEEE/ASME Trans. Mechatronics*, vol. 21, no. 5, pp. 2440–2452, Oct. 2016.
[24] H. Khalil, Nonlinear Systems, *3rd ed*. Englewood Cliffs, NJ, USA: Prentice-Hall, 2002.
[25] M. Krstic, I. Kanellakopoulos, and P. Kokotovic, Nonlinear and Adaptive Control Design, Hoboken, NJ, USA Wiley, 1995.
[26] W. Kim, D. Won, D. Shin, and C. C. Chung, "Output feedback nonlinear control for electro-hydraulic systems," *Mechatronics*, vol. 22, no. 6, pp. 766–777, 2012.
[27] Z. P. Jiang and L. Praly, "Design of robust adaptive controllers for nonlinear systems with dynamic uncertainties," *Automatica*, vol. 34, no. 7, pp. 825–840, 1998.

Wonhee Kim (Member, IEEE) received the B.S. and M.S. degrees in electrical and computer engineering and the Ph.D. degree in electrical engineering from Hanyang University, Seoul, South Korea, in 2003, 2005, and 2012, respectively.

From 2005 to 2007, he was with Samsung Electronics Company, Suwon, South Korea. In 2012, he was with the Power and Industrial Systems Research and Development Center, Hyosung Corporation, Seoul, South Korea. In 2013, he was a Postdoctoral Researcher with the Institute of Nano Science and Technology, Hanyang University, Seoul, South Korea, and a Visiting Scholar with the Department of Mechanical Engineering, University of California, Berkeley, CA, USA. From 2014 to 2016, he was with the Department of Electrical Engineering, Dong-A University, Busan, South Korea. He is currently an Associate Professor with the School of Energy Systems Engineering, Chung-Ang University, Seoul, South Korea. His current research interests include nonlinear control and nonlinear observers, as well as their industrial applications.

Dr. Kim has served as an Associate Editor for the IEEE/ASME TRANSACTIONS ON MECHATRONICS, the IEEE ACCESS, AND THE JOURNAL OF ELECTRICAL ENGINEERING & TECHNOLOGY.

Youngwoo Lee received the B.S. degree from Chungbuk National University, Cheongju, Korea, in 2010, and the Ph.D. degree from Hanyang University, Seoul, Korea, in 2017, both in electrical engineering.

From 2017 to 2018, he was a Research Scientist with the Ulsan National Institute of Science Technology, and a Visiting Scholar with the Department of Mechanical Engineering, University of California, Berkeley, CA, USA. From 2018 to 2019, he was with the Memory Division, Samsung Electronics Ltd., Korea. From 2019 to 2020, he was an Assistant Professor with the Department of Electronics Engineering, Pai Chai University, Daejeon, Korea. In 2020, he joined the Faculty of Chonnam National University, Gwangju, Korea. His main research interests include nonlinear and optimal controller design, motion control.

Donghoon Shin received the B.S. degree in electrical and computer engineering and the Ph.D. degree in electrical engineering from Hanyang University, Seoul, Korea, in 2009 and 2016, respectively.

He is a Senior Research Engineer with Global R&D Center, Mando Co., Korea. His main research interests include nonlinear control and observer as well as their industrial applications.

Chung Choo Chung (Member, IEEE) received the B.S. and M.S. degrees in electrical engineering from Seoul National University, Seoul, South Korea, in 1981, and the Ph.D. degree in electrical and computer engineering from the University of Southern California, Los Angeles, CA, USA, in 1983 and 1993, respectively.

Before the Ph.D. program, he worked for L.G. Electronics and IBM Korea. From 1994 to 1997, he was with the Samsung Advanced Institute of Technology, Korea, where he was selected as a Samsung Group 21 C Leader. He also finished the Samsung Advanced Management Program at the Wharton School of the University of Pennsylvania in 1996. In 1997, he joined the Faculty of Hanyang University, Seoul, South Korea.

Dr. Chung was an Associate Editor for various journals such as *Asian Journal of Control*, IEEE TRANSACTIONS ON CONTROL SYSTEM TECHNOLOGIES, IEEE TRANSACTIONS ON INTELLIGENT TRANSPORTATION SYSTEMS, and a Founding Editor for the *International Journal of Control, Automation, and Systems*, and now an Associate Editor for the IFAC Mechatronics. He also served as an Associate or a Senior Editor for various international conferences, including IEEE CDC, ACC, IFAC WC, IEEE IV, IEEE ITSC. He was a Guest Editor for TCST, 2012, and also for the IEEE Intelligent Transportation Systems Magazine, 2017. He was a General Chair of IEEE CDC 2020.